M.O.11 Technical Note (B) No.15

Truncation errors in the finite different solution of the vorticity advection equation - some numerical assessments.

By J. S. Sawyer.

1. Introduction.

In solving the differential equations of numerical forecasting truncation errors necessarily occur, but little information is available on their magnitude. It was therefore decided to solve the simple equation for the advection of vorticity using as an initial stream function an analytical field which should progress without change of form if the equation were correctly solved. Errors in the solution could then be assessed.

The vorticity advection equation which has been solved is

$$\nabla^2 \frac{\partial \psi}{\partial t} = J(\nabla^2 \psi, \psi) \quad - \quad - \quad (1)$$

where ψ is a stream function such that $u = -\partial\psi/\partial y$, $v = \partial\psi/\partial x$. This is similar to the equation used in numerical forecasts with the barotropic model except that the terms arising from the variation of the coriolis parameter with latitude have been dropped for simplicity. They are not likely to affect the character or magnitude of the errors.

Finite differences are used in ~~solveney~~ solving (1) both to evaluate the operator $\nabla^2 \equiv \partial^2/\partial x^2 + \partial^2/\partial y^2$ and to evaluate the Jacobian $\equiv J(a,b) \equiv \frac{\partial a}{\partial x}\frac{\partial b}{\partial y} - \frac{\partial a}{\partial y}\frac{\partial b}{\partial x}$

Since ∇^2 appears on both sides of the equation the errors in approximating ∇^2 on the two sides of the equation tend to balance out. Thus errors in evaluating the first derivatives which make up the Jacobian are probably more serious as contributing to the total error of the calculation, because no corresponding derivatives in x and y appear on the left hand side of the equation.

The type of error arising from truncation error in the Jacobian has been studied by Knighting (1), Gates (2), Obukhov (3) and Okland (4) in regard to the simpler equation.

$$\frac{\partial q}{\partial t} = U \frac{\partial q}{\partial x}$$

which represents simple advection with velocity U along the x - axis. (Wippermann(s) also gives a similar discussion of truncation error in a linearised form of the vorticity advection equation).

When equation (2) is written in finite difference form

$$\frac{q_{t+1} - q_{t-1}}{2\Delta t} = U \frac{q_{n+1} - q_{n-1}}{2\Delta x} \quad - \quad - \quad - \quad (2)$$

and applied to a sinusoidal disturbance

$$q(x) = A \sin \frac{2\pi x}{L} \quad - \quad - \quad - \quad (3)$$

it is shown by these authors that the solution can be written

$$q(x,n) = P \sin\left(\frac{2\pi x}{L} - n\lambda\right) + Q \sin\left(\frac{2\pi x}{L} + n\lambda + n\pi\right) \quad - \quad - (4)$$

where $$\sin\lambda = \frac{U\Delta t}{\Delta x} \sin \frac{2\pi \Delta x}{L}$$

The first term in (4) represents a progressive wave approximately to the true solution of (2). The second term which tends to zero as $\Delta x, \Delta t \to 0$ is entirely fictitious.

The solution is bounded (stable) provided $U\Delta t/\Delta x < 1$ (Courant-Friedrichs-Lewy criterion) and the speed of the progressive wave is given by

$$c_1 = \frac{L}{2\pi\Delta t} \sin^{-1}\left(\frac{U\Delta t}{\Delta x} \sin\frac{2\pi\Delta x}{L}\right) \qquad \text{—— — (5)}$$

This underestimates the speed of the wave. The underestimation increases - as the wavelength decreases, becoming substantial when L is reduced to $4\Delta x$.

The stream functions to which we wish to apply equation (1) are not simple sinusoidal functions but can be regarded as made up of a spectrum of different wavelengths. The individual components will, however, appear to have different speeds when integration is made from an equation such as (3). This "false dispersion" has been commented on by Økland (4) as a cause of distortion of the troughs and ridges in the predicted flow in numerical forecasts and is responsible for the "parasitic waves" found by Obukhov (3) when equation (2) was applied to a simple step-function.

More accurate finite difference approximations have been considered. In particular, Økland (4) demonstrates that a five-point difference relation for $\partial q/\partial x$ in (2) gives a closer estimate of the velocity of the disturbance and reduces the false dispersion. Equation (3) then becomes

$$\frac{q_{r+1} - q_{r-1}}{2\Delta t} = U\,\frac{8(q_{n+1} - q_{n-1}) - (q_{n+2} - q_{n-2})}{12\,\Delta x}$$

and the velocity of the disturbance computed from it is

$$c_2 = \frac{L}{2\pi\Delta t} \sin^{-1}\left(\frac{U\Delta t}{\Delta x}\left\{\frac{\sin\frac{2\pi\Delta x}{L}\left(4 - \cos\frac{2\pi\Delta x}{L}\right)}{3}\right\}\right) \qquad \text{— (6)}$$

The criterion for stability is now somewhat more restrictive namely $U\Delta t/\Delta x < 0.73$. These theoretical results form a basis for comparison with the solutions of (1) by finite difference methods.

2. The computing programme.

A programme (TES) was written for the computer METEOR to carry out numerical integration of equation (1) by the finite difference methods normally used in numerical forecasting. Thus the operator ∇^2 was approximated by ∇ where

$$\nabla q_{r,s} = \frac{1}{(\Delta x)^2}\left\{q_{r+1,s} + q_{r,s+1} + q_{r-1,s} + q_{r,s-1} - 4q_{r,s}\right\}$$

and the first derivations which occur in the Jacobian were approximated by the simple formula

$$\frac{\partial q_{r,s}}{\partial x} = \frac{q_{r+1,s} - q_{r-1,s}}{2\Delta x} \qquad etc$$

In addition the programme provided facilities to try three more complicated finite difference approximations to the Jacobian in equation (1), namely:-

(a) a five point formula to the first derivatives

(b) Bickley's formula for the first derivatives

(c) Pedersen's formula for the Jacobian.

(a) The five point formula to the x-derivative (suggested by Okland(4)) is

$$\frac{\partial q_{r,s}}{\partial x} = \frac{8(q_{r+1,s} - q_{r-1,s}) - (q_{r+2,s} - q_{r-2,s})}{12\Delta x}$$

Together with the corresponding formula for the y-derivative this was used to evaluate $J(\nabla^2\psi, \psi)$ in (1).

(b) Bickley (6) gives an alternative form for the first derivative namely

$$\frac{\partial q}{\partial x}_{r,s} = \frac{1}{12\Delta x}\left\{4(q_{r+1,s} - q_{r-1,s}) + q_{r+1,s+1} - q_{r-1,s+1} + q_{r+1,s+1} - q_{r-1,s-1}\right\} - \frac{(\Delta x)^2}{6}\nabla\left(\frac{\partial q}{\partial x}\right)_{r,s}$$

The second term on the right hand side is evaluated from the approximate value of $\partial q/\partial x$ given by the first term on the right-hand side alone. $J(\nabla^2\psi, \psi)$ was evaluated using the Bickley formula for both the x- and y-derivatives.

(c) Pedersen (7) recommends an alternative finite difference approximation to the Jacobian, J(a,b) namely

$$\left[J(a,b)\right]_{r,s} = \frac{1}{3(\Delta x)^2}\left\{(a_{r+1,s} - a_{r-1,s})(b_{r,s+1} - b_{r,s-1}) - (a_{r,s+1} - a_{r,s-1})(b_{r+1,s} - b_{r-1,s})\right\}$$

$$- \frac{1}{48(\Delta x)^2}\left\{(a_{r+2,s} - a_{r-2,s})(b_{r,s+2} - b_{r,s-2}) - (a_{r,s+2} - a_{r,s-2})(b_{r+2,s} - b_{r-2,s})\right\}$$

The finite difference form of equation (1) was applied to the field

$$\psi = \psi_0\left(2 - \frac{1}{1 + \frac{x^2+y^2}{a^2}} - \frac{y}{b}\right)$$

This stream function represents a circular vortex superimposed on a uniform stream and the analytical solution of equation (1) shows the pattern of stream lines displaced steadily in the x-direction with a velocity $1/b$

The programme provides for either

(a) boundary values made equal to the true solutions of (1)

(b) boundary values constant.

The solution was carried out on a 19 x 19 grid of points, the boundary conditions being applied at the outer two rows of points.

The Poisson equation for $\nabla^2(\partial\psi/\partial t)$ was solved by an iterative Liebmann process, the iterations being continued until both

(a) the change in ψ/ψ_0 at all points was numerically less than 2^{-15}

(b) the (algebraic) total residual was less than 2^{-9}

The initial step in the time integration was made using uncentred time differences as is usual in numerical forecasting procedure.

All of the results discussed below were obtained using the boundary values obtained from the true solution of (1).

3. Results.

The results of the numerical integrations are conveniently discussed in times of the parameters a and b of the initial field and of a third parameter c used to specify the time increment in the time integration. a is the radius at which the disturbance of the stream function from the basic stream has half its value at the centre of the vortex. The basic stream has a velocity $1/b$ (the unit of distance being the grid length). $c = \Delta t/b$ is the fraction of a gridlength moved by the system in the time increment.

Experiments were conducted with values of a of 8, 4, 2 and 1. If the grid length were 300Km as in current experiments a = 4 corresponds to a half radius of 1200Km - the circulation represented thus corresponds to a large depression. a = 2 would correspond to a small depression and a = 1 to a very small system but nevertheless within the scale of disturbances which do occur.

In terms of the parameter c and the wavelength, L , the theoretical speeds for the calculated movement of a sinusoidal disturbance may be rewritten from equations (5) and (6) thus:-

simple difference approximation

$$\frac{\text{Calculated speed}}{\text{True speed}} = \frac{U_p}{U_A} = \frac{L}{2\pi c} \sin^{-1}\left(c \sin \frac{2\pi}{L}\right)$$

5-point difference approximation

$$\frac{\text{Calculated speed}}{\text{True speed}} = \frac{U_p}{U_A} = \frac{L}{2\pi c} \sin^{-1}\left(\frac{c}{3} \sin \frac{2\pi}{L}\left(4 - \cos \frac{2\pi}{L}\right)\right)$$

The variation of the expressions (7) and (8) with L for c = 0·25 is illustrated in Fig.1.

The ratio of calculated motion to true motion is also shown for features of the stream functions fields in the numerical calculations by finite difference methods. This is shown both in respect of the trough-line and of the centre of maximum vorticity. These were obtained by comparing the initial and final stream functions after 16 time steps which should altogether have displaced the stream function pattern by 4 gridlengths. The values of the ratio for numerical integration is plotted against the parameter a on a scale which equates L = 4a.

(a) The simple (3-point) finite difference formula.

The most noteworthy feature of the results of the numerical integrations applied to the larger scale patterns a = 4 and a = 8 was the underestimate of the movement of the features of the stream function field. As the scale of the stream function field is decreased there is an increasing tendency to distort the stream function field, to displace the maximum of vorticity to the right of its proper path and to "fill up" the centre of the vortex. With a = 2 and a = 1 noteworthy irregularities were generated in the stream function field outside the immediate field of the vortex. These features can largely be interpreted in terms of the proceeding theoretical results and will be discussed separately below.

(i) Speed of vortex

The speed of the trough-line in the stream function field was calculated to be greater than that of the vorticity maximum in each case - both being underestimates of the correct velocity. This is understandable because the position of the trough line is determined by larger scale Fourier components of the stream function pattern than is the vorticity and the former are expected to be displaced with a speed closer to the correct value.

The fact that the curves in Fig.1 for the numerical integrations slope less steeply than the theoretical curves is to be explained in a similar way. For the larger scale vortices the position of the troughline is determined by smaller scale features than those which determine the profile of the trough at a distance from the axis, but as the width of the trough is reduced in terms of the grid length the smallest scale features cannot be resolved and the important wavelength in fixing the trough line becomes bigger in relation to the trough width.

Since the calculated speed of the longer wavelength is greater than that of the smaller, the calculated speed decreased less rapidly with the scale of the trough than predicted by theory for sinusoidal waves.

With the stream function pattern assumed, the maxima of the vorticity advection ahead and behind the trough occur at $x = \pm \cdot 35a$. Thus a representative wavelength for the vorticity pattern in the neighbourhood of the trough might be set at $L = 4a/3$. The calculated speeds of the vorticity maxima for a = 8 and a = 4 agree roughly with the theoretical on this basis.

The theoretical results in equation (7) and (8) suggest that the error magnitude will largely be independent of b if c remains the same. One calculation with a = 2 b = 4 c = 0·25 gave slightly larger proportional errors in velocity than one using a = 2, b = 8 c = 0·25 - the computed trough speed as a fraction of the true speed being 0·80 against 0·86 in the latter case. The result is however a little unreliable because integration was taken only to 8 time steps and placing the computed troughline with sufficient accuracy was not easy.

(ii) False dispersion.

The effect of "false dispersion" arising because component wavelengths are moved with different speeds is illustrated in Fig.2 after 16 time steps by the profile of the stream function through the vortex centre in the direction of the advection. The calculated and true profiles are shown for a = 2. The effect of the "false dispersion" is to increase the minimum value of the stream function and to make the gradient of ψ steeper in the rear of the minimum than ahead of it. A secondary effect arising from the stronger transverse flow behind the centre than ahead is to create a displacement of the vortex to the right of the general stream. This was apparent in all the computations and the displacement increased from very small values with a = 8 to 1/4 of the true displacement with a = 1. Fig.2 also illustrates the underestimate of the trough speed.

(iii) Parasitic waves.

The effect of truncation error in producing fictitious waves is shown most markedly with the smallest-scale trough for which the calculation was performed (namely a = 1). Here the vortex was largely defined by the value at one point (the centre) and four surrounding points. The profile of ψ through the centre (Fig.3) clearly shows the parasitic waves in addition to the other truncation error effects already discussed. Although the Courant-Friedrichs-Lewy critical velocity was just exceeded at one grid point in the initial field it is unlikely that the irregularities arise from computational instability of the usually recognised type. The irregularities also appear if the time-step is shortened so that the criterion for stability is satisfied and can also be traced in the computation with a = 2 (also stable according to the Courant-Friedrichs-Lewy criterion).

Figs. 4, 5, 6 and 7 show the initial field of ψ, the final field of ψ and the error field for a = 4 and a = 1 (In both cases b = 8, c = 0·25 and 16 time steps have been carried out). The pattern in Figures 4 and 6 should have been displaced 4-grid lengths to the right if the results of the computation had been free from truncation error.

(iv) Effect of change of time step.

The equations (7) and (8) suggest that an increase in the time step (increase in c) will reduce the truncation error provided that the condition for computational stability is not exceeded. The expressions (7) and (8) are however not very sensitive to changes in c within the possible range. The result is however complicated by the uncentred differences used at the first time step.

An integration carried out to eight time steps with c = 0·5 (a = 4, b = 8) gave almost identical results with one carried to sixteen time steps with c = 0·25 although the Courant-Frierichs-Lewy criterion for stability was just exceeded at a small group of points on the lower side of the trough line.

(b) The five point formula.

As would be expected the use of the 5-power formula in computing the first derivatives in the 'advection Jacobian' leads to a significant reduction in errors. The estimate of the speed of the troughline is improved and the error is very slight except with the smallest scale of vortex ($a = 1$). The effect of false dispension in distorting the profile of the vortex is negligible and the displacement of the vorticity centre to the right of its proper track is very small except for the smallest scale ($a = 1$). With the smaller scale vortices the apparent filling of the centre is still present and also the "parasitic waves". Compared with the results using the simple (3-point) formula the "filling of the centre" is materially reduced for $a = 2$, but there is little difference in respect of $a = 1$. The amplitude of the parasitic waves are about the same whether the 3-point or 5-point formula is used.

The ratio of the computed and correct speed, of the troughline are shown in Fig.1, and Fig.8 illustrates the computed profile of ψ for the smallest vortex ($a = 1$) using the 5-point formula. Figs.9 and 10 give results for ($a = 4$) and ($a = 1$) for comparison with Figs.5 and 7 obtained on the same data with the 3-point formula.

(c (A computation using the 4-point formula with $a = 4$, $b = 8$ and $c = 0{\cdot}5$ showed substantial sinusoidal irregularities probably arising from computational instability. This is consistent with the fact that the appropriate criterion for stability was exceeded by a maximum of about 50%. The corresponding computation using the two the two point formula showed no computational instability but in this case the advecting velocity exceeded the theoretical maximum for stability by about 10% and at a group of 6 points only.

(c) Bickleys formula.

The results of using Bickley's formula for the derivatives are very close to those obtained using the five-point formula, and do not merit separate discussion. The maximum errors were generally slightly greater with Bickley's formula than with the 5-point formula.

(d) Pedersen's formula.

The results of using Pedersen's formula for the Jacobian were also very similar to those obtained with the 5-point formula. Again the errors were generally slightly greater.

(e) Calculations on an alternative stream function.

Similar integrations of equation (1) were also carried out with the initial stream function given by

$$\psi = \left(-Ae^{x/a}\sin\frac{\pi y}{k} + \frac{x}{d} + \frac{y}{b}\right)\psi_0$$

This provided some confluence and diffluence such as occurs in association with the jet stream. Again the correct solution of equation (1) should have indicated a motion of the ψ -field without change of form.

Using $A = 0{\cdot}125$, $a = 8$, $b = -8$, $k = 8$, $d = -16$ and $c = 0{\cdot}25$ the results again showed that use of the 3-point formula tended to underestimate the motion of the system. When the 5-point formula for the first derivative was used errors were reduced to little more than 1/10 of their previous values over much of the area of integration.

Table I gives a complete list of the calculations made and some measures of their accuracy.

4. Discussion.

The present experiments demonstrate that truncation errors in numerical forecasts are not negligible and that with features of the flow pattern comparable with large depressions the errors in the computed displacement using the usual 3-point approximation to the first derivative may amount to more than 10%. It appears that this error can be substantially reduced by the use of a five-point approximation, but the requirements of computational stability are then rather more restrictive. It is also seen that disturbances of the stream pattern with dimensions of 2 to 4 grid lengths are very badly treated whichever approximation is used. The presence of such small scale features will also introduce errors outside their immediate neighbourhood because truncation errors lead to spurious small scale features superimposed on the true solution. There is therefore a strong argument in favour of smoothing or filtering out the very short wavelength features before the integration is started.

5. Some barotropic forecasts with the 5-point approximation.

Four barotropic forecasts of 500 mb. height have been made using the 5-point approximation to the derivatives in the Jacobian in place of the usual simple 3-point formula. The forecasts were based on stream functions derived for the 500 mb. level and was carried to 24-hours.

Systematic differences between the forecasts using 3-point and 5-point finite difference approximations were not large. Differences of 30 to 40 m existed however over some areas with dimensions of several grid-lengths. The largest individual difference at a grid point was 100m. Some verification statistics are given in Table I.

Table I - Comparison of verification statistics for forecast based on 3-point and 5-point finite difference approximations.

Date	3-point					5-point				
	a	b	c	d	e	a	b	c	d	e
		m		kt.			m		kt.	
5 Feb., 1959	0·91	72	0·67	24	0·73	0·91	71	0·68	24	0·71
10 Feb., 1959	0·89	101	0·41	40	0·51	0·89	106	0·40	41	0·48
17 Feb., 1959	0·94	97	0·79	29	0·74	0·93	101	0·77	30	0·71
3 Mar., 1959	0·93	82	0·68	30	0·81	0·93	80	0·69	29	0·84

Column a - correlation between forecast and verifying charts

b - r.m.s. height error

c - correlation between forecast and actual height changes

d - r.m.s. vector wind error

e - correlation between forecast and actual geostrophic wind.

As expected the use of the 5-point formula gave significantly greater displacement of mobile troughs and ridges by some 10 to 15%. In general this did not make any material difference to the accuracy of the forecasts because the trough and ridge positions were subject to much larger errors from other causes (the selected examples were all cases of substantial forecast errors). However a clear improvement was effected in respect of a small trough over the British Isles in the forecast of 3 March 1959. There were also some other small scale features which were clearly treated better by the 5-point formula than the 3-point, but the 3-point formula gave noticeably smoother results - the 5-point formula results containing a number of minor irregularities which did not correspond to features of the actual charts.

The forecasts based on the 5-point formula gave systematically lower values than those using the 3-point formula over much of the chart - the average difference overall was 10m. This may be due to the closer approximation to the vorticity advection in an area generally between the trough over East America and the ridge over Europe.

The statistical verification of the forecasts shows no significant difference between the two integration procedures. The local improvement in some areas introduced by the 5-point formula has been masked by the increased irregularities introduced into the pattern.

Acknowledgements.

The barotropic forecasts reported in section 5 were carried out by Miss M.K. Hinds. Much of the programming required in the investigation was done by Mr. J. Langley.

REFERENCES

(1) E. Knighting and D.E. Jones. Finite difference approximations in numerical forecasting. Moll Technical Note (B) No.7 1958.

(2) W. L. Gates. On the truncation error, stability and convergence of difference solutions of the barotropics vorticity equation. J. Met. Vol.16, 1959 p.556.

(3) A.M. Obukhov. On the accuracy of calculation of advective changes in numerical prediction of the weather. Moscow. Ak. Nauk. Izv. Ser. Geof. 1957 p.1133.

(4) H. Økland. False dispersion as a source of integration error. Scientific Report No.1. Det. Norske. Met. Inst. Oslo 1958.

(5) F. Wippermann. Uber das Verhalten des Truncation fehlers bei Verwendang der zweidimensionalen und divergenzfrein Vorticity-diffenzengleichung. Met. Rundschan Vol.8, 1955 p.44.

(6) W.G. Bickley. Finite difference formulae for the square lattice. Q.J. Mech. and Applied Math. Vol.1, 1948, p.36.

(7) K. Pederson. A discussion of errors in finite difference operators substituted for the Laplace operator and the Jacobian. Rapport Nr.2 Videnskaps - Akademiets Institutt for Vaer-og klimaforshnig, Oslo, 1959.

TABLE I

Summary of results using TES Programmes.

Correct boundary conditions.

Data Number	a	b	c	N number of time-steps	Max error x 10^3	Trough speed / correct speed
Three point formula						
1	4	8	0·25	16	-45	0·925
7	8	8	0·25	16	- 7	0·94
5	2	8	0·25	16	-178	0·86
6	1	8	0·25	16	+547	0·82
2	2	4	0·25	8	-110	0·80
8	4	8	0·5	8	-47	0·925
Five-point formula						
3	4	8	0·25	16	- 9	0·99
12	2	8	0·25	16	+63	1·00
14	1	8	0·25	16	+451	0·95
15	4	8	0·5	8	+65	1·0
Bickleys formula						
3	4	8	0·25	16	-12	0·99
11	2	8	0·25	16	-92	0·99
13	1	8	0·25	16	+465	0·95
16	4	8	0·5	8	+216	0·97
Pedersens formula						
1	4	8	0·25	16	- 9	0·99
5	2	8	0·25	16	+65	0·99
6	1	8	0·25	16	+433	0·95

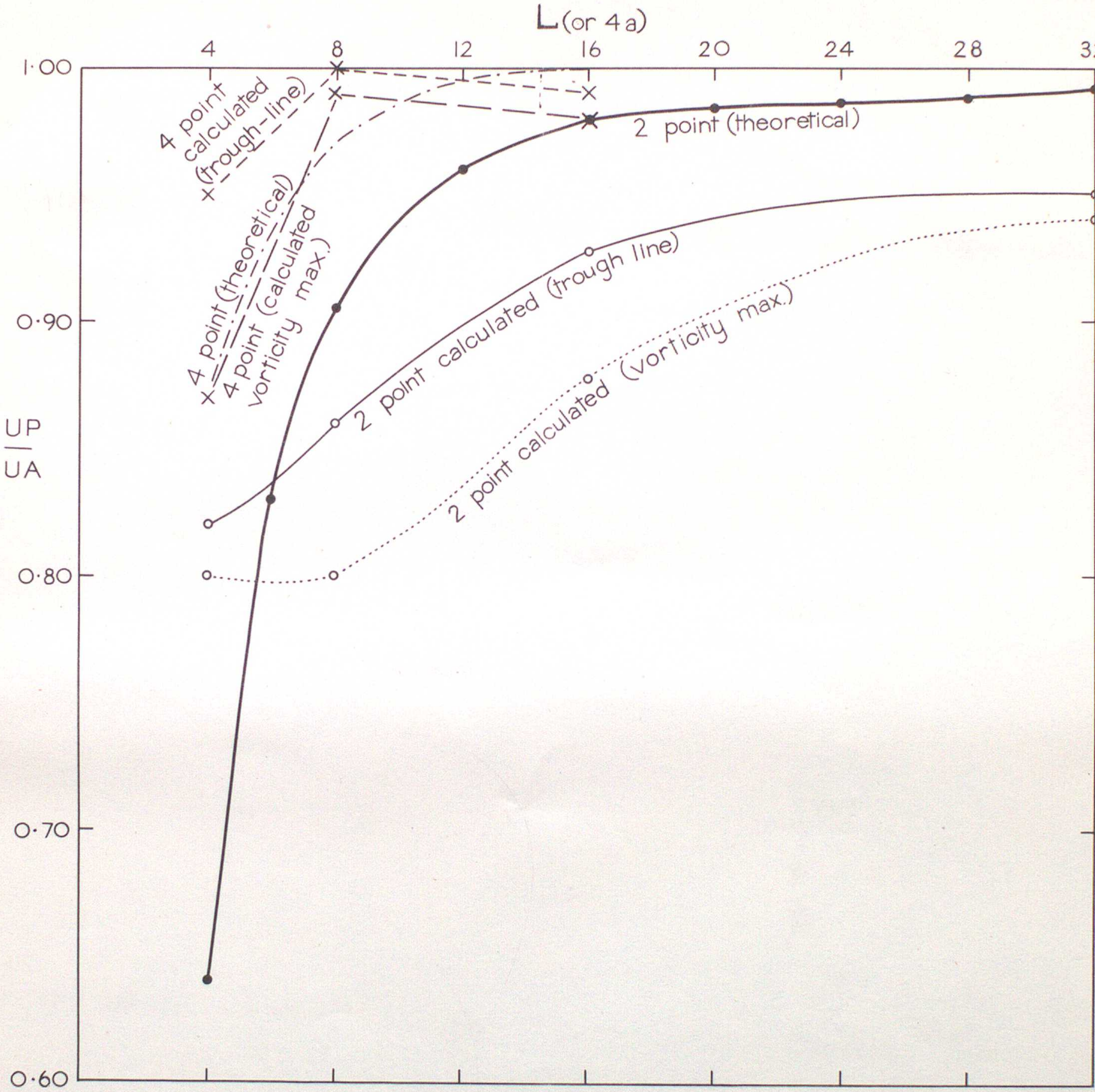

Fig. 1. Ratio of calculated to true speed of trough in relation to scale of disturbance

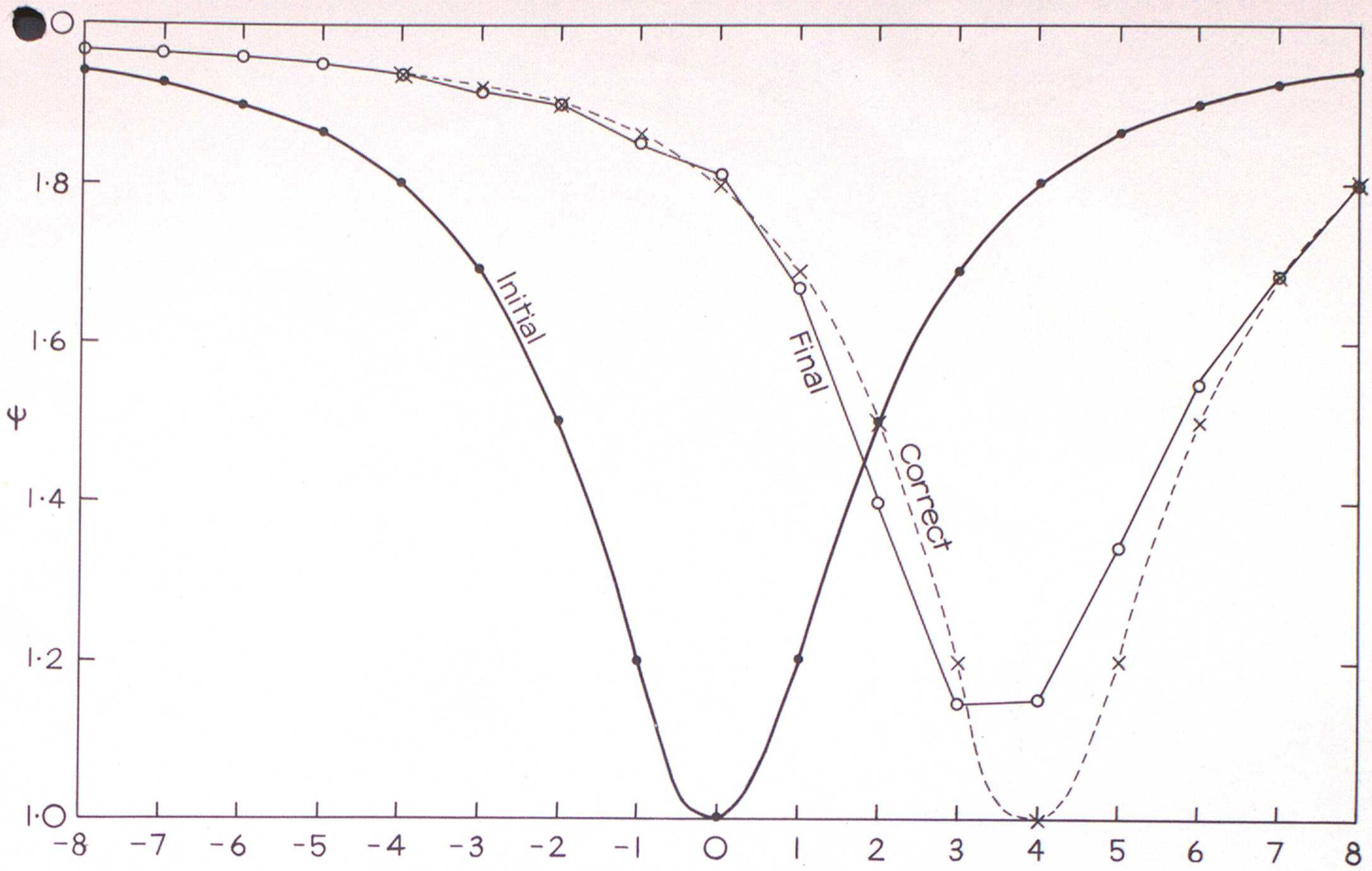

Fig. 2. Profile of ψ as calculated for a=2, b=8, c=0·25 (16 time steps)

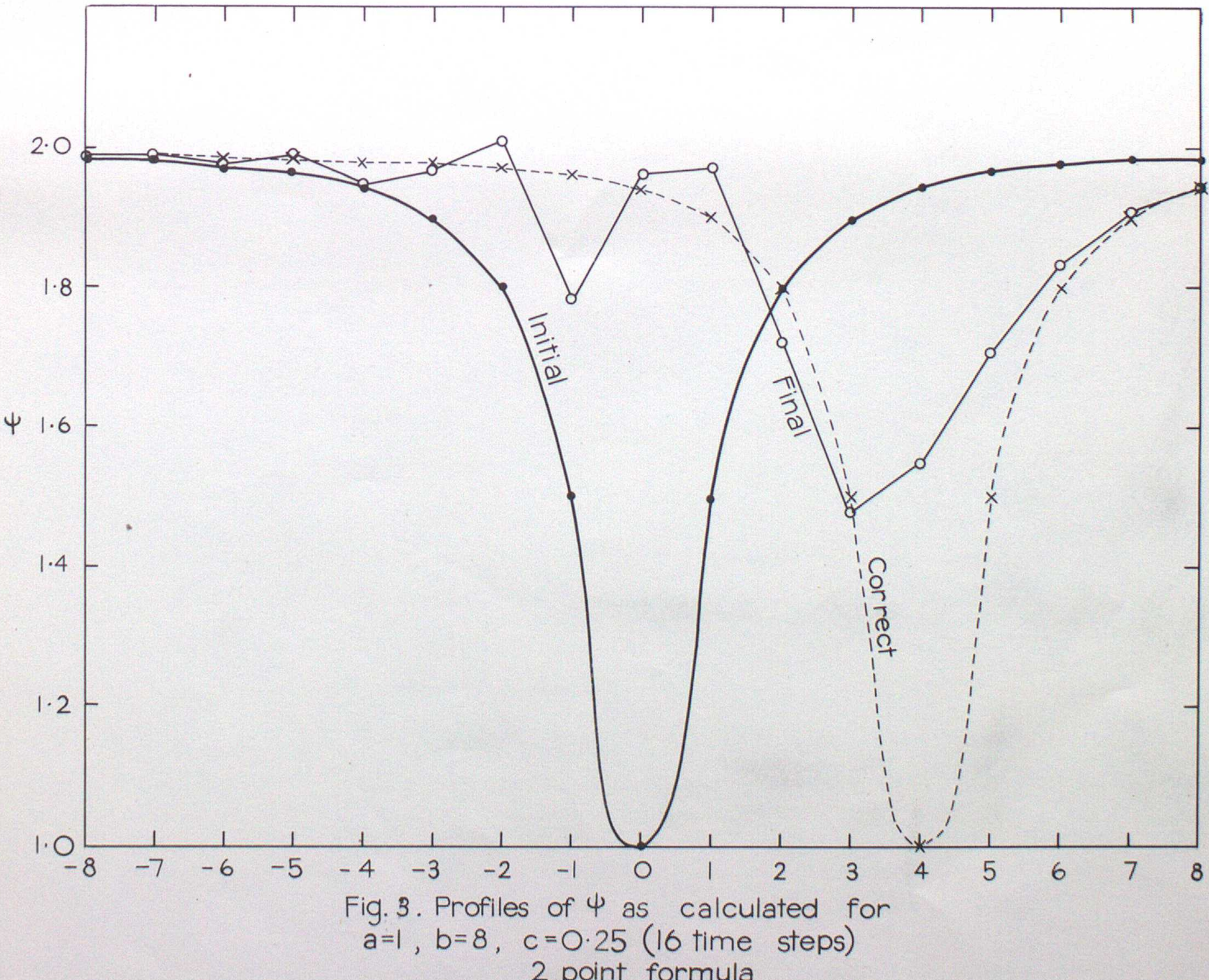

Fig. 3. Profiles of ψ as calculated for a=1, b=8, c=0·25 (16 time steps) 2 point formula

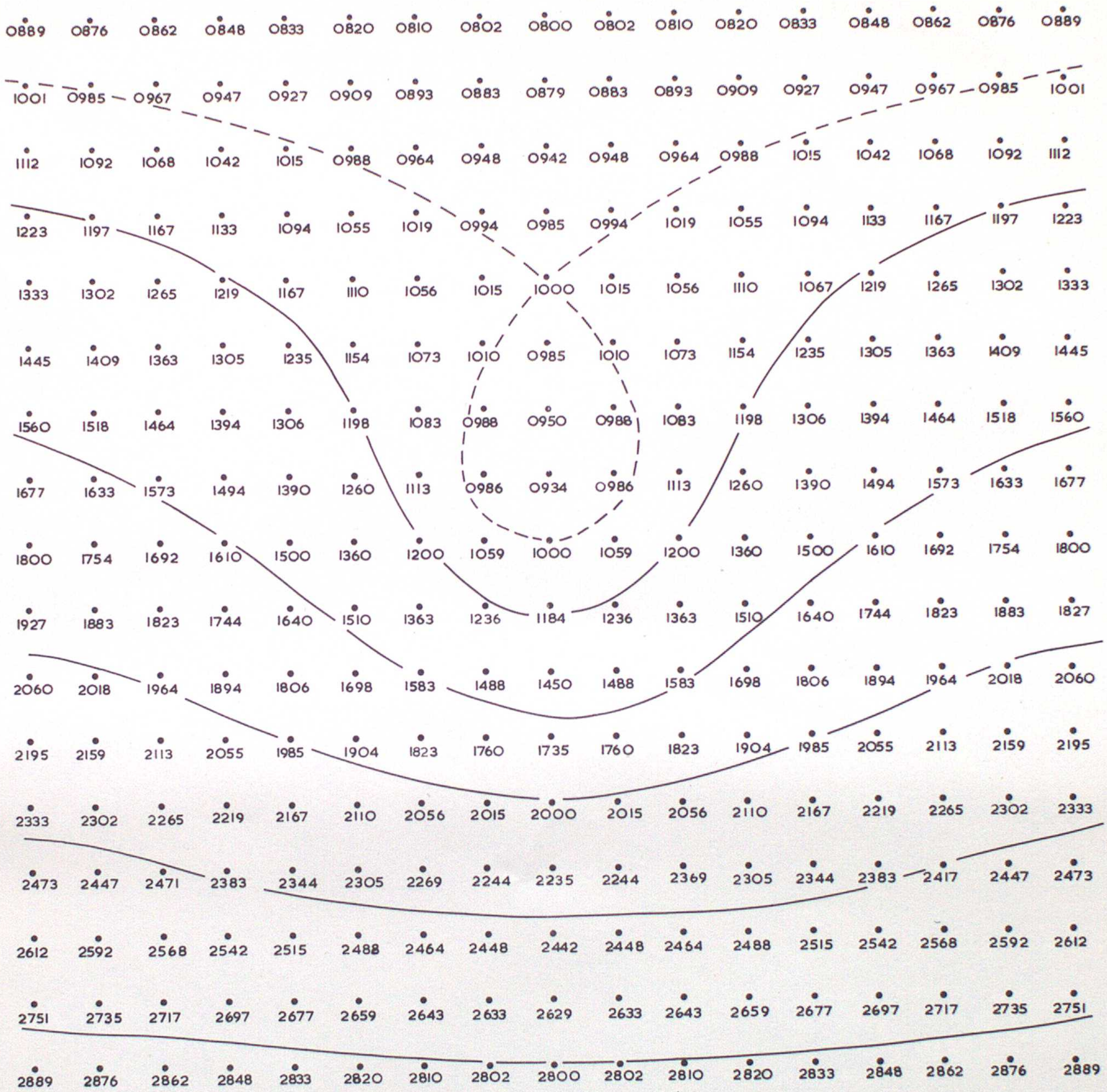

Fig. 4. Initial field Ψ/Ψ_0

$a = 4$, $b = 8$.

All figures are multiplied by 10^3

929 −0	920 0	911 0	901 0	889 0	876 0	862 0	848 0	833 0	820 0	810 −0	802 −0	800 −0	802 −0	809 −0	820 −0	833 −0
1048 −0	1039 0	1028 0	1015 0	1001 0	985 0	967 0	947 0	927 0	909 −0	893 −0	882 −0	879 −0	882 −0	893 −0	909 −0	927 −0
1168 −0	1158 0	1145 0	1130 0	1112 −0	1092 −0	1068 −0	1042 −0	1015 −0	987 −0	964 −0	948 −1	942 −0	948 −0	964 0	988 0	1015 −0
1288 −0	1276 0	1262 −0	1244 0	1223 −0	1197 −0	1167 −0	1132 −0	1094 −1	1054 −1	1018 −1	993 −1	985 −0	995 1	1021 1	1056 1	1094 −0
1409 −0	1395 0	1379 −0	1358 0	1333 0	1302 −0	1264 −0	1218 −1	1165 −2	1107 −2	1053 −1	1014 −1	1002 2	1019 4	1060 4	1112 3	1167 −0
1530 0	1515 −0	1497 −0	1474 0	1445 0	1409 0	1362 −1	1303 −2	1231 −4	1148 −6	1067 −6	1008 −1	992 7	1021 11	1083 9	1159 5	1235 0
1652 −0	1636 −0	1617 0	1592 0	1560 1	1518 0	1463 −1	1391 −4	1298 −7	1186 −13	1070 −13	986 −2	965 15	1010 22	1100 17	1205 7	1306 0
1776 −0	1759 −0	1738 0	1712 1	1678 1	1633 1	1572 −1	1489 −5	1379 −11	1237 −22	1087 −26	978 −8	954 20	1018 32	1137 23	1267 8	1390 0
1900 −0	1883 0	1862 0	1836 1	1801 1	1755 1	1693 1	1607 −3	1488 −12	1330 −30	1157 −43	1033 −25	1012 +12	1091 32	1226 26	1370 10	1500 0
2026 −0	2009 0	1989 0	1963 1	1929 1	1884 2	1825 2	1747 3	1637 −3	1487 −23	1318 −45	1197 −39	1178 −6	1257 21	1386 23	1522 12	1640 0
2152 −0	2137 0	2117 0	2092 1	2061 2	2021 2	1967 3	1899 5	1812 6	1692 −6	1554 −29	1452 −36	1434 −16	1495 7	1598 14	1710 11	1806 0
2280 −0	2266 0	2247 0	2225 1	2197 2	2162 3	2115 3	2060 5	1998 6	1907 3	1808 −15	1734 −26	1718 −17	1759 −1	1830 7	1912 8	1985 0
2409 −0	2396 0	2379 0	2359 1	2335 1	2305 2	2267 2	2223 4	2173 0	2112 2	2046 −9	1998 −17	1987 −13	2012 −4	2057 2	2114 4	2167 −0
2538 −0	2526 0	2512 0	2492 1	2474 1	2449 2	2419 2	2385 3	2347 3	2305 −0	2263 −7	2234 −10	2226 −9	2241 −4	2269 −0	2307 +2	2344 −0
2668 −0	2658 0	2645 0	2630 0	2613 1	2593 1	2569 1	2544 1	2516 1	2487 −1	2460 −4	2442 −6	2437 −5	2446 −3	2463 −1	2488 1	2515 −0
2798 −0	2789 0	2778 0	2766 0	2751 0	2735 1	2717 1	2698 1	2678 0	2658 −1	2641 −2	2630 −3	2627 −2	2631 −1	2643 −1	2659 0	2677 −0
2929 −0	2920 0	2911 0	2901 0	2889 0	2876 0	2862 0	2848 0	2833 0	2820 0	2810 0	2802 −0	2800 −0	2802 −0	2809 −0	2820 −0	2833 −0

Fig. 5. Final field of Ψ/Ψ_0 and error field (two-point formula)

$a=4$ $b=8$ $c=0{\cdot}25$ 16 steps.

All figures multiplied by 10^3. Errors plotted as lower figures.

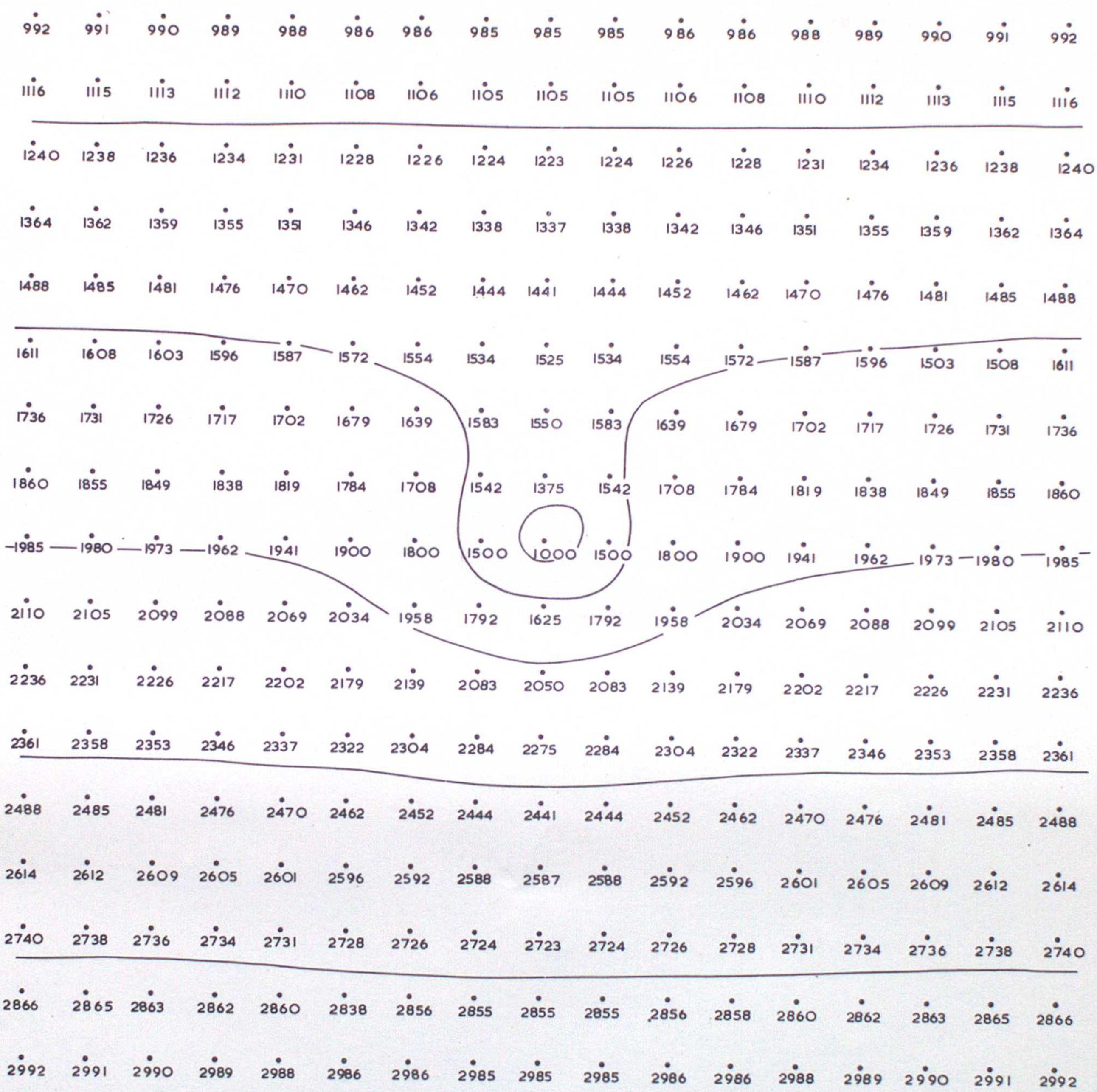

Fig. 6. Initial field Ψ/Ψ_0

$a=1$, $b=8$.

All figures multiplied by 10^3.

995	995	994	993	992	991	990	989	988	986	986	985	985	985	986	986	988
−0	−0	0	0	0	0	0	0	0	0	−0	−0	−0	−0	−0	−0	−0
1120	1119	1117	1116	1114	1112	1110	1109	1108	1107	1107	1107	1107	1107	1108	1109	1110
−0	−0	−1	−2	−2	−3	−3	−3	−2	−1	0	1	2	2	1	1	−0
1244	1243	1240	1238	1235	1232	1230	1228	1227	1227	1227	1227	1227	1227	1229	1230	1231
−0	−1	−2	−4	−5	−6	−7	−6	−4	−1	1	3	4	4	3	2	−0
1369	1367	1364	1360	1356	1351	1348	1345	1344	1345	1345	1343	1343	1344	1347	1350	1351
−0	−1	−3	−6	−8	−10	−11	−11	−0	−2	3	6	7	6	5	4	0
1494	1491	1487	1482	1476	1470	1464	1459	1457	1459	1459	1454	1452	1455	1461	1467	1470
−0	−2	−5	−8	−12	−15	−17	−18	−13	−2	6	10	11	11	9	6	0
1618	1615	1610	1604	1596	1587	1578	1566	1564	1571	1566	1550	1543	1553	1568	1581	1587
−0	−2	−6	−10	−15	−21	−26	−30	−23	−1	12	16	18	19	14	9	0
1743	1740	1734	1728	1713	1711	1681	1668	1654	1684	1662	1608	1594	1623	1661	1690	1702
−0	−2	−7	−10	−22	−20	−44	−49	−48	5	23	25	44	40	22	12	0
1868	1864	1862	1841	1873	1758	1915	1662	1749	1834	1753	1583	1573	1657	1740	1794	1820
0	−3	−3	−22	14	−97	66	−176	−70	50	45	42	198	115	31	10	0
1993	1991	1983	1993	1952	1978	2012	1784	1965	1974	1722	1482	1547	1709	1835	1906	1941
−0	−1	−7	5	−33	−2	+39	−177	23	74	−78	−18	547	209	35	6	0
2118	2118	2109	2137	2046	2210	2090	1894	2207	2245	1808	1548	1668	1854	1978	2041	2070
−0	1	−6	24	−63	104	−8	−194	137	211	−151	−244	43	62	20	7	0
2243	2243	2242	2250	2225	2296	2233	2184	2426	2446	2041	1835	1896	2014	2109	2168	2202
−0	1	1	12	−10	65	8	−32	224	267	−98	−248	−154	−69	−30	−11	0
2368	2369	2370	2373	2372	2391	2381	2384	2485	2471	2260	2148	2162	2213	2264	2303	2337
−0	1	4	9	10	33	27	37	148	149	−413	−136	−113	−71	−39	−19	0
2494	2494	2495	2498	2501	2508	2510	2519	2546	2526	2440	2384	2376	2394	2420	2441	2470
−0	1	4	8	13	23	29	43	76	65	12	−61	−66	−51	−32	−18	−0
2619	2619	2621	2623	2625	2629	2632	2636	2641	2626	2589	2560	2550	2556	2569	2583	2601
−0	1	4	7	11	17	23	31	39	29	−2	−28	−36	−32	−23	−14	0
2744	2745	2745	2747	2748	2750	2751	2753	2751	2742	2725	2711	2704	2705	2712	2719	2731
−0	1	3	5	8	12	15	19	20	14	−0	−13	−19	−18	−14	−9	−0
2870	2870	2870	2870	2870	2871	2871	2870	2869	2864	2857	2850	2847	2847	2850	2854	2860
−0	0	1	3	4	6	7	9	0	6	0	−5	−8	−8	−6	−4	−0
2995	2995	2994	2993	2992	2991	2990	2989	2988	2986	2986	2985	2985	2985	2986	2986	2988
−0	0	0	0	0	0	0	0	0	0	0	−0	−0	−0	−0	−0	−0

Fig. 7 Final field Ψ/Ψ_0 and error field (two point formula)

a=1, b=6, c=0·25, 16 steps.

All figures multiplied by 10^3. Errors plotted as lower figures.

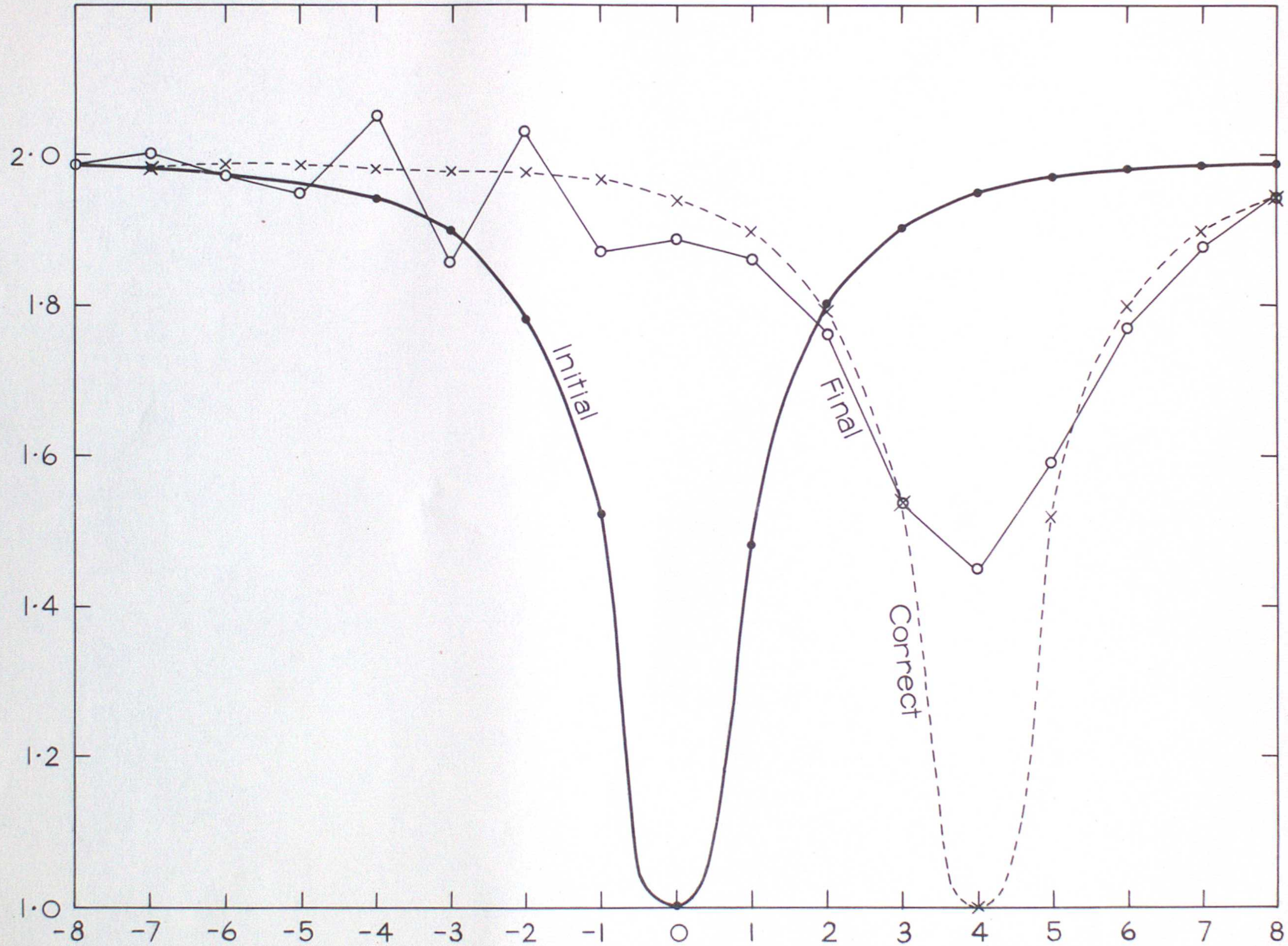

Fig. 8 Profiles of ψ as calculated for
$a=1$, $b=8$, $c=0{\cdot}25$ (16 time steps)
4 point formula

929 -0	920 0	911 0	901 0	889 0	876 0	862 0	848 0	833 0	820 0	810 -0	802 -0	800 -0	802 -0	809 -0	820 -0	833 -0
1048 -0	1039 0	1028 0	1016 0	1001 0	985 0	967 0	948 0	928 0	909 0	893 0	882 -0	878 -1	882 -1	893 -1	908 -0	927 -0
1168 -0	1158 0	1145 0	1130 0	1112 0	1092 0	1069 1	1043 1	1015 1	988 1	964 0	948 -1	941 -1	947 -1	963 -1	987 -1	1015 -0
1288 0	1276 0	1262 0	1244 0	1223 1	1198 1	1168 1	1133 1	1095 1	1056 1	1020 0	993 -1	983 -2	992 -2	1018 -1	1054 -1	1094 -0
1409 -0	1395 0	1379 0	1359 0	1334 1	1303 1	1266 1	1220 1	1168 1	1111 1	1056 0	1014 -1	998 -2	1014 -2	1055 -1	1109 -0	1167 -0
1530 -0	1515 -0	1497 0	1475 1	1446 1	1410 1	1364 1	1306 1	1236 1	1155 1	1073 -0	1009 -1	984 -1	1009 -1	1073 0	1154 -0	1235 0
1652 -0	1636 -0	1617 0	1592 1	1561 1	1519 1	1465 0	1394 -0	1306 0	1199 0	1083 -0	988 0	952 2	989 1	1084 0	1197 -2	1306 0
1776 -0	1759 0	1739 0	1713 1	1679 1	1633 1	1573 -1	1493 -1	1390 -0	1259 -0	1112 -1	986 0	938 4	989 3	1114 1	1256 -4	1390 0
1900 -0	1883 0	1863 1	1836 1	1801 1	1754 0	1692 -1	1608 -2	1499 -1	1359 -1	1195 -5	1053 -5	1000 +0	1060 1	1202 2	1356 -4	1500 0
2026 -0	2009 0	1989 0	1963 1	1928 1	1883 0	1823 -0	1743 -1	1641 1	1511 1	1360 -3	1227 -9	1177 -6	1233 -3	1363 -0	1507 -2	1640 0
2152 -0	2137 0	2117 0	2092 1	2060 0	2019 1	1965 1	1895 0	1807 2	1702 4	1586 2	1484 -4	1444 -6	1484 -4	1582 -1	1697 -1	1806 0
2280 -0	2266 0	2247 0	2225 1	2196 0	2159 1	2114 1	2056 1	1986 1	1908 3	1828 4	1760 0	1732 -3	1756 -4	1822 -1	1904 -0	1985 0
2409 -0	2396 0	2379 0	2359 0	2334 0	2303 1	2366 1	2221 1	2168 1	2112 2	2058 3	2015 0	1997 -3	2013 -3	2055 -1	2110 0	2167 -0
2538 -0	2526 0	2512 0	2494 0	2473 0	2448 1	2418 1	2383 1	2245 1	2306 1	2270 1	2243 -1	2233 -2	2243 -2	2269 -1	2305 -0	2344 -0
2668 -0	2658 0	2645 0	2630 0	2612 0	2592 0	2569 1	2543 1	2515 0	2488 0	2464 -0	2447 -1	2441 -1	2447 1	2464 -0	2488 0	2515 -0
2798 -0	2779 0	2778 0	2766 0	2751 0	2735 0	2717 0	2698 0	2678 0	2659 0	2643 -0	2632 -0	2628 -0	2632 -0	2643 -0	2659 -0	2677 -0
2929 -0	2920 0	2911 0	2901 0	2889 0	2876 0	2862 0	2848 0	2833 0	2820 0	2810 0	2802 -0	2800 -0	2802 -0	2809 -0	2820 -0	2833 -0

Fig. 9. Final field of Ψ/Ψ_0 and error field (four-point formula)
a=4, b=8, c=0·25. 16 steps.
All figures multiplied by 10^3 Errors plotted as lower figures.

0995 -0	0995 -0	0994 0	0993 0	0992 0	0991 0	0990 0	0989 0	0988 0	0986 0	0986 -0	0985 -0	0985 -0	0985 -0	0986 -0	0986 -0	0988 -0
1120 -0	1119 -0	1117 -1	1116 -2	1114 -2	1113 -2	1112 -2	1111 -1	1111 2 or 0	1110 2	1110 4	1110 5	1110 5	1110	1110 3	1110 2	1110 -0
1244 -0	1243 -1	1241 -2	1238 -4	1236 -5	1234 -5	1232 -4	1232 -2	1232 2 or 0	1233 5	1233 8	1233 10	1233 10	1233 10	1233 7	1233 5	1231 -0
1369 -0	1367 -1	1364 -4	1359 -6	1356 -8	1353 -9	1352 -7	1352 -4	1352 1	1354 7	1354 13	1354 16	1354 17	1354 16	1353 12	1355 8	1351 0
1494 -0	1491 -2	1486 -6	1480 -10	1475 -13	1471 -14	1469 -12	1469 -7	1469 -0	1472 10	1471 19	1469 25	1468 27	1470 26	1470 18	1474 12	1470 0
1618 -0	1614 -3	1609 -7	1598 -16	1594 -17	1583 -25	1583 -20	1584 -12	1581 -6	1587 14	1581 28	1569 35	1566 41	1573 39	1580 27	1589 17	1587 0
1743 -0	1741 -1	1720 -20	1731 -7	1688 -47	1723 -9	1668 -58	1710 -7	1680 -22	1696 18	1669 30	1628 45	1619 69	1644 61	1675 36	1699 20	1702 0
1868 -0	1854 -13	1887 +22	1796 -67	1898 38	1743 -112	1853 5	1749 -89	178 -37	1825 41	1784 76	1601 60	1578 203	1646 104	1737 29	1796 12	1820 0
1993 -0	2001 9	1975 -16	1957 -31	2053 69	1857 -123	2047 75	1872 -89	1884 -58	1861 -39	1761 -39	1534 34	1451 451	1592 92	1769 -31	1880 -20	1941 0
2118 -0	2143 26	2043 -32	2145 32	2128 18	1995 -110	2233 134	2064 -24	1842 -228	1868 -166	1891 -68	1661 -130	1514 -111	1647 -145	1849 -109	1981 -53	2070 0
2243 -0	2249 7	2213 -28	2256 17	2238 2	2198 -33	2308 83	2226 10	2048 -154	2066 -112	2236 97	2189 105	1999 -51	1962 -121	2056 -83	2128 -50	2202 0
2368 -0	2368 0	2360 -6	2367 3	2364 2	2356 -3	2380 27	2354 7	2287 -50	2297 -25	2405 101	2422 138	2310 35	2252 -32	2272 -32	2295 -27	2337 0
2494 -0	2492 -0	2490 -2	2490 0	2489 2	2488 3	2490 9	2480 3	2461 -8	2469 7	2508 55	2519 74	2481 39	2447 3	2444 -8	2449 -12	2470 0
2619 -0	2618 -0	2616 -1	2616 0	2615 1	2614 3	2613 4	2609 4	2604 3	2609 13	2623 31	2626 38	2613 27	2597 9	2593 1	2592 -4	2601 0
2744 -0	2743 -0	2742 -0	2742 0	2741 1	2740 2	2739 3	2737 3	273 5	2738 10	2743 17	2744 20	2739 16	2731 8	2729 3	2727 -1	2731 -0
2870 -0	2869 -0	2868 -0	2867 0	2867 0	2866 1	2865 1	2864 2	2863 3?	2863 5	2864 8	2864 9	2862 7	2859 4	2858 2	2858 -0	2860 -0
2995 -0	2995 0	2994 0	2993 0	2992 0	2991 0	2990 0	2989 0	2988 0	2986 0	2986 0	2985 -0	2985 -0	2985 -0	2986 -0	2986 -0	2988 -0

Fig. 10. Final field of Ψ/Ψ_0 and error field (four-point formula)
$a=1$, $b=8$, $c=0\cdot25$, 16 steps.
All figures multiplied by 10^3. Errors plotted as lower figures.